Thermomagnetic irreversibility in $Ni_2Mn_{1.36}Sn_{0.64}$ shape-memory alloy

S. Chatterjee, S. Giri, and S. Majumdar*
Department of Solid State Physics, Indian Association for the Cultivation of Science, 2A & B Raja S. C. Mullick Road, Jadavpur, Kolkata 700 032, India

S. K. De
Department of Materials Science, Indian Association for the Cultivation of Science, 2A & B Raja S. C. Mullick Road, Jadavpur, Kolkata 700 032, India

(Received 11 April 2008; revised manuscript received 12 May 2008; published 27 June 2008)

The ferromagnetic shape-memory alloy of nominal composition $Ni_2Mn_{1.36}Sn_{0.64}$ has been investigated by electronic transport and magnetic studies. The thermoelastic martensitic transition is strongly influenced by the applied magnetic field as observed in our resistivity and magnetization measurements. The field-cooled and the zero-field-cooled resistivities show large divergence below the transition temperature. It is evident that the field cooling through the martensitic transition produces a fraction of arrested austenitic phase, which persists even down to the lowest temperature of measurement. The field-cooled resistivity shows large relaxation signifying the nonequilibrium character of the state. The close interplay between magnetization and the structural phase of the sample plays important role toward the formation of this undercooled arrested state. A parallelism is drawn between the field-induced anomalies observed in the present shape-memory alloy and some manganites showing insulator-metal transition.

DOI: 10.1103/PhysRevB.77.224440 PACS number(s): 75.60.Nt, 81.30.Kf, 75.30.Kz

I. INTRODUCTION

The coupling between magnetic and structural degrees of freedom in a solid can lead to intriguing physical properties, which have immense importance both from fundamental and technological point of views. In case of many intermetallic alloys and compounds, magnetic field-induced structural transition is responsible for various functional behaviors such as giant magnetocaloric effect,[1] colossal magnetostriction,[2] magnetic superelasticity,[3,4] giant magnetoresistance[5–7] etc. Some striking properties of the perovskite based manganese oxides also originate from magnetostructural instabilities.[8] As a result of the first-order nature of the transition, metastable states are formed,[9] and the system can show fascinating dynamics resulting from the competition between thermal and magnetic energies. Considering the growing interests in various systems showing magnetostructural instabilities, it is pertinent to understand the thermomagnetic behavior of systems with such competing interactions.

Heusler based ferromagnetic shape-memory alloys (FSMAs)[10] are interesting *biferroic* materials showing both ferroelasticity (development of spontaneous strain) and ferromagnetism (development of spontaneous magnetization). Recently, $Ni_2Mn_{1+x}Sn_{1-x}$ based FSMAs have attracted considerable attention due to their remarkable magnetofunctional properties such as shape-memory effect, inverse magneto caloric effect, and giant magnetoresistance around the martensitic transition (MT).[11–14] These are primarily related to the field-induced structural transition, which has been confirmed by x-ray diffraction experiment.[14] Application of magnetic field near MT induces a reverse transition, where the martensitic fraction transforms into austenite. This transition was found to be highly irreversible in most of the $Ni_2Mn_{1+x}Sn_{1-x}$ alloys i.e., one cannot recover the transformed fraction by simply withdrawing the field. Recently, we observed interesting *return point memory effect* in $Ni_2Mn_{1.4}Sn_{0.6}$ arising from the field arrested austenite state.[13] Formation of a field-induced low-temperature glassy magnetic state has been reported for the isostructural indium alloy.[15] Evidently, these materials are an ideal system for studying the effect of H and T variation across the MT. The present investigation was performed on the polycrystalline sample of nominal composition $Ni_2Mn_{1.36}Sn_{0.64}$ and it is mainly based upon the detailed magnetotransport studies on the alloy. $Ni_2Mn_{1.36}Sn_{0.64}$ contains less manganese than our previously studied sample $Ni_2Mn_{1.4}Sn_{0.6}$ and it has much lower value of the martensitic transition temperature. We observe intriguing history dependence with respect to the parameters, H and T, manifesting magnetically arrested states, which posses a remarkable resemblance with some manganites showing first-order insulator-metal transition.

II. EXPERIMENTAL DETAILS

The polycrystalline sample of composition $Ni_2Mn_{1.36}Sn_{0.64}$ was prepared by argon arc melting and subsequent annealing. The room-temperature powder x-ray diffraction pattern confirms that the material is a single-phase alloy with $L2_1$ cubic structure having lattice parameter, $a = 5.99$ Å. The magnetization (M) was measured by Quantum Design SQUID magnetometer (MPMS 6, Ever-cool model). The resistivity (ρ) was measured using a commercial cryogen free high magnetic-field system from Cryogenic Ltd., U.K. in the temperature (T) range 5–300 K and in presence of magnetic field 0–90 kOe. The sample space of the system is always filled up with He exchange gas for good thermal stability and the temperature fluctuation was less than 20 mK during the isothermal measurements.

III. RESULTS

Figure 1 shows the ρ versus T data recorded at 0 and 50 kOe of field with different protocols. In the zero-field data

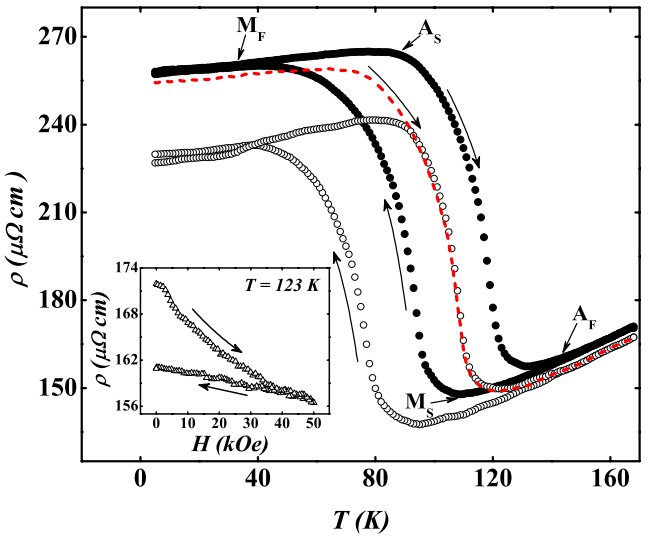

FIG. 1. (Color online) Resistivity as a function of temperature at zero field (filled circles) and 50 kOe field (open circles) for both cooling and subsequent heating sequences. The dashed line indicates resistivity measured by heating the sample at 50 kOe of field after the sample being zero-field-cooled down to 5 K. The inset shows the resistivity at 123 K for both field increasing and decreasing branches.

(filled circles), clear thermal hysteresis is observed between the heating and cooling measurements in the range 35–155 K, signifying the first-order MT in the alloy. For an applied magnetic field (H) of 50 kOe, the field cooling and subsequent field-heating data (open circles) show similar thermal hysteresis, however, now the high-T end point of the loop is shifted to lower temperatures along with the lowering of the magnitude of ρ. This is related to the field-induced transition near the magnetostructural instability and gives rise to magnetoresistance (MR) as large as −30%. Notably, $\rho(T)$ (open circles) measured in $H=50$ kOe during field cooling and field heating do not approach the zero-field data (filled circles) below the MT, rather they remain *well below* in magnitude and run parallel to the zero-field data and considerable MR (−12%) is observed down to the lowest temperature of measurement. The MR arising from the magnetostructural transition is likely to be observed in the vicinity of the MT. However, for the present sample, it appears that the reduced value of ρ in presence of H is carried over well below the region of thermal hysteresis. This is a magnetothermal arrest of the low-ρ phase, which remains arrested even when the sample is cooled below the MT and subsequently heated back in field. Now let us look at the zero-field-cooled but field-heating data (dashed line), where the sample was heated from 5 to 300 K in $H=50$ kOe after being zero-field-cooled to 5 K. Here, $\rho(T)$ is almost same to that of the zero-field run below the MT, decreases considerably as it enters into the region of thermal hysteresis and then above the MT, it again approaches the zero-field data. We therefore observe a large deviation between the field-cooled field-heating (open circles) and zero-field-cooled field-heating (dashed line) data measured at $H=50$ kOe. The deviation starts to emerge from 90 K, which is well inside the region of thermal hysteresis.

We have recorded isothermal ρ versus H data at 123 K (inset of Fig. 1), where a clear irreversibility is observed

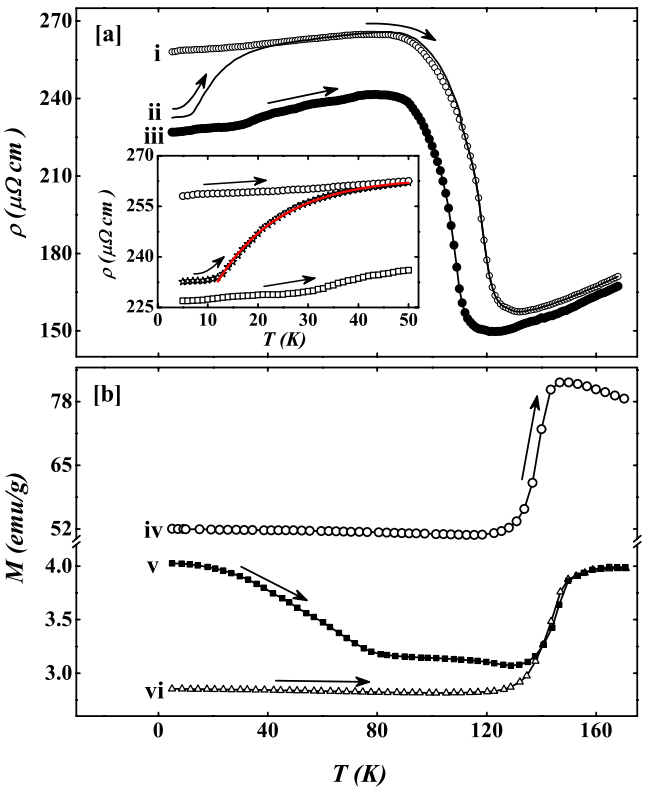

FIG. 2. (Color online) (a) Resistivity recorded while heating in (i) zero field after being zero-field cooled, (ii) zero field after being field cooled in $H=50$ kOe and (iii) 50 kOe after being field-cooled in $H=50$ kOe. (b) Magnetization recorded while heating in (iv) 50 kOe after being field cooled in 50 kOe, (v) 100 Oe of field after being field cooled in $H=50$ kOe (vi) 100 Oe of field after being field cooled in 100 Oe.

between the field increasing and decreasing branches. The application of field brings down ρ, however, when the field is ramped down to zero, ρ remains arrested in its *low value* state. The irreversibility in $\rho(H)$ is actually the manifestation of irreversibility of the magnetostructural transition of the sample. The observed anomaly in the field-cooled ρ versus T emerges out of this field induced arrest of the low-ρ state, which remains arrested even when the sample is cooled down to 5 K.

In order to shed more light on this interesting thermomagnetic behavior, we collected heating $\rho(T)$ and $M(T)$ data with different protocols as depicted in Fig. 2. $\rho(T)$ was recorded in varied conditions, such as (i) zero-field-cooled (ZFC) and then zero-field heating, (ii) field-cooled (FC) in $H=50$ kOe and zero-field heating, (iii) cooled in $H=50$ kOe and heating in 50 kOe. Starting from the lowest T, curve (iii) remains well separated from curve (i), which is the effect of field cooling across the magnetostructural transition. If we look at curve (ii), it also remains well below curve (i) [rather close to curve (iii)] at the lowest temperature. However, above about 10 K (see the inset for a zoomed view), it starts to approach curve (i) and eventually joins up with it above 50 K. It depicts that the field cooling produces a *nonequilibrium* state which persists even when the field is removed at the lowest temperature, nevertheless it tends to the *equilibrium* ZFC

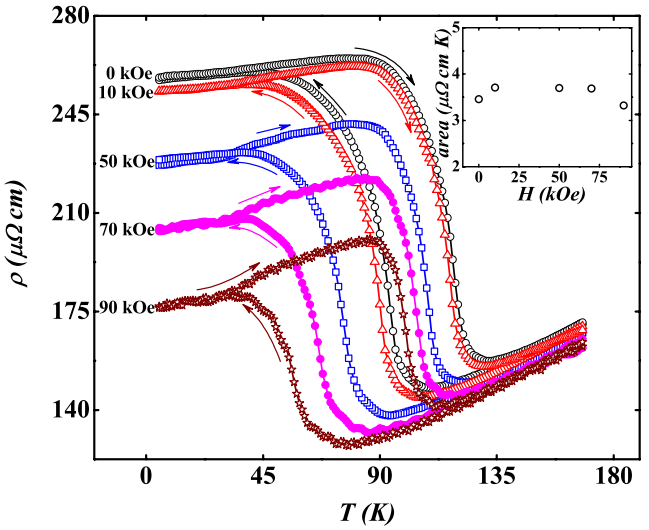

FIG. 3. (Color online) Field cooling and field-cooled heating resistivity data measured at different applied fields. The inset shows the area of the thermal hysteresis loops as a function of H.

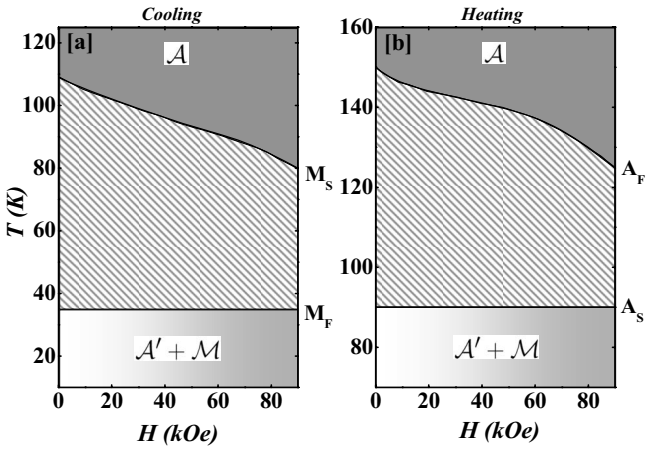

FIG. 4. The H-T phase diagram of the sample for cooling and heating in a field H. Here, $\mathcal{A}$ denotes the high-temperature phase, $\mathcal{M}$ is the martensite phase, and $\mathcal{A}'$ is the field arrested undercooled austenite phase. The stripes (between M_S and M_F in case of cooling and between A_F and A_S in heating) denote the region of thermoelastic martensitic transition.

state once we increase the temperature. Interestingly, curve (ii) shows an exponential behavior as it approaches curve (i) [a fitted line is shown in the inset of Fig. 2(a)], with an empirical law of temperature dependence: $\rho(T)=A-B\exp(-T/T_0)$, here A, B, and T_0 are fitting parameters. Our fitting to the data gives T_0 to be 12 K, which is very close to the temperature from where curve (ii) starts to rise. This shows that field cooling in 50 kOe produces a metastable state which is separated from the equilibrium state by a barrier of height of about 12 K.

The magnetization data also show similar field-cooling effect. In Fig. 2(b), curves (iv) and (v) are measured while heating in $H=50$ kOe and 100 Oe, respectively, after both being field-cooled in 50 kOe. In case of curve (vi), the sample was field cooled in 100 Oe and $M(T)$ was measured in 100 Oe during heating. Therefore, the magnetization curves (iv), (v), (vi) are equivalent to the resistivity curves (iii), (ii), (i), respectively, except only the fact that instead of zero field, M was measured in a low field of 100 Oe. We find strong effect of field cooling, as the curves (v) and (vi) differ from each other. The difference is maximum at the lowest temperature, but as the sample is warmed up, curve (v) approaches curve (vi), signifying the unblocking of the field arrested state under heating in low field (100 Oe).

Figure 3 shows $\rho(T)$ measured at different fields with hysteresis loops consisting of field-cooling and field-heating branches. Our $\rho(T)$ measurement up to the field strength of 90 kOe indicates that thermally driven MT survives till such a high field, but it is strongly modified by the metamagnetic transition. Grossly, the loop shifts to lower T with increasing H. MT is characterized by four temperatures, namely M_S, M_F while cooling, and A_S and A_F while heating. Martensite starts to develops from M_S and the transition completes at M_F. Similarly, A_S and A_F signify austenite start and finish temperatures, respectively, while heating. Roughly, M_F and A_F are low-T and high-T end points of the hysteresis loop, while M_S is the minimum point and A_S is the maximum point in the T-decreasing and T-increasing branches (marked in Fig. 1) of the ρ versus T data. With the application of H, M_S shifts to lower T and for 0 to 90 kOe of field change, $\Delta M_S=33$ K. Similarly, we observe $\Delta A_F=30$ K. M_F and A_S remain almost constant under an applied magnetic field. The magnitude of ρ gets suppressed below A_F under H and the hysteresis loop becomes fatter but shorter with increasing H. Interestingly, the area under the thermal hysteresis loops remain almost constant for different applied fields (see inset of Fig. 3).

It is clear from the previous data that the field cooling produces a state with lower ρ and higher M than the ZFC state. The sample has been reported to show martensite to austenite transformation under H. Considering the fact that austenite is electrically less resistive and having higher magnetic moment than martensite, the field cooling through MT actually produces some austenite fraction, which survives even when the sample is cooled below the martensite finish temperature, M_F. As a result, the FC resistivity decreases with increasing field, signifying the development of more and more arrested austenite fraction with increasing H. Figure 4 shows the H-T phase diagram of the sample for cooling and subsequent heating in a field H. In the cooling data, the line M_S separates the pure austenite and the low-temperature mixed phase occurring due to the thermoelastic MT. The line M_F, which indicates the end of thermoelastic transition, is found to be insensitive to the cooling field. Below this line, the arrested austenite ($\mathcal{A}'$) is indicated by shades, which increases with increasing H. On the heating H-T diagram [Fig. 4(b)], the existence of the arrested austenite, $\mathcal{A}'$ is indicated below the starting point of the thermoelastic transition, A_S. We observe that unlike M_S and A_F, the characteristic temperatures A_S and M_F hardly change with changing field. This is possibly due to the fact that the effect of H is to create arrested austenite out of metastable martensite only, and the martensite phase is metastable between the temperatures M_S and A_F.

A metastable state is defined as a state corresponding to the local minimum in the free-energy configuration separated

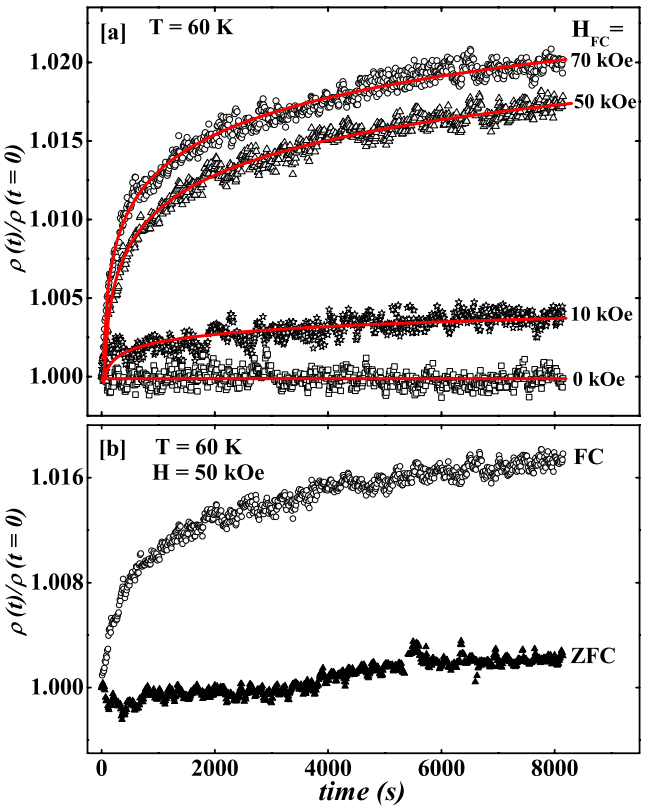

FIG. 5. (Color online) (a) The upper panel depicts normalized resistivity as a function of time at 60 K. The relaxation measurements were performed after the sample was field cooled in a particular field H_{FC} down to 5 K, heated back to 60 K, and then removing the field H_{FC}. The solid lines are the logarithmic fit to the data. (b) Relaxation of resistivity at 60 K for two different protocols, namely FC, where the sample was field cooled in $H=50$ kOe down to 5 K, heated back to 60 K and relaxation was measured by removing the field, and ZFC, where the sample was zero-field-cooled down to 5 K and at this temperature 50 kOe of field was applied and the sample was allowed to heat up to 60 K, and then the relaxation was measured by removing the field.

by an energy barrier from the equilibrium state. For $T \neq 0$, the thermal energy can assist the system to evolve into the equilibrium configuration. It is therefore interesting to see how the resistivity in the arrested FC state relaxes with time (t). Figure 5(a) depicts the relaxation of ρ as a function of time at 60 K. The sample was field cooled to 5 K in $H=H_{FC}$, heated back to 60 K in the same field and then ρ was measured as a function of time after the removal of the field H_{FC}. Once the field is removed, ρ quickly attains a value close to the zero-field resistivity, $\rho_{H=0}$ [curve (i) of Fig. 2]. On the heating branch, 60 K is a temperature that is too high to keep the austenite arrested completely. After that it sluggishly increases toward $\rho_{H=0}$ with t. We measured $\rho(t)$ for about 8000 s, and a reasonably large relaxation in ρ was observed (about 2.1% for $H_{FC}=70$ kOe). In our measurement, $t=0$ denotes the time when the field is completely removed. In all cases ρ increases with t and it asymptotically approaches the zero-field value. The sluggish rise of ρ for $t>0$ depends strongly upon H_{FC}, and it is clearly seen that the relaxation is more prominent for higher H_{FC}. This is not surprising because a higher value of H_{FC} will create a higher fraction of arrested metastable state. At zero applied field, the sample does not show any relaxation due to the absence of field-induced metastability. We observe a logarithmic evolution of ρ with time: $\rho(t)/\rho(t=0)=1+S_\rho \ln(t/t_0)$, where t_0 and S_ρ are the fitting parameters [solid lines in Fig. 5(a)]. A logarithmic relaxation of physical parameters is well established and it can happen due to the thermal excitation of the system across the distribution of energy barriers.[16] The coefficient of the logarithmic term, S_ρ, increases sharply with increasing H_{FC}.

One can argue that the observed relaxation is simply due to the finite reaction time of a ferromagnetic sample such as $Ni_2Mn_{1.36}Sn_{0.64}$ to the removal of a magnetic field. In order to rule out the possibility, we measured the relaxation of ρ at 60 K after removing the field (50 kOe) for both FC and ZFC protocols [see Fig. 5(b)]. In case of FC, the sample was field-cooled in 50 kOe down to 5 K and heated back to 60 K in field, while in ZFC case, the sample was zero-field-cooled down to 5 K, 50 kOe field was applied and then heated back in field to 60 K. Clear signature of relaxation is observed in case of FC state, while for the ZFC case, the relaxation is insignificant. It signifies that the field cooling through the MT has distinctive effect on the electronic state of the system. A mere application of field below 60 K on the ZFC state cannot produce the nonequilibrium state, which can relax with time.

IV. DISCUSSION

The present system is an interesting example where we observe a mutual coexistence of thermally driven MT and the field driven reverse transition, both first order in nature, which together give rise to a complex H-T behavior. Similar interplay between two orderings are observed in other systems such as multiferroic materials (ferromagnetic and ferroelectric)[17] and intermetallic alloy such as $ZrZn_2$,[18] where superconductivity and ferromagnetism coexist. However, as far as the magnetothermal properties are concerned, $Ni_2Mn_{1.36}Sn_{0.64}$ shows remarkable similarities with the manganite compounds, $(Nd,Sm)_{0.5}Sr_{0.5}MnO_3$.[8,19] Here, the temperature driven first-order ferromagnetic (FM) to charge-order (CO) transition gets shifted to lower temperature with the applied magnetic field, which signify a field-induced reverse CO to FM transition. Consequently, H tries to stabilize the FM phase and a field-cooling through the first-order CO-FM transition (which is also associated with a insulator-metal transition) gives rise to metastable metallic FM fraction below the region of thermal hysteresis (see Fig. 1 of Ref. 19) that persists down to the lowest temperature. The development of this FM phase due to the field cooling in case of $(Nd,Sm)_{0.5}Sr_{0.5}MnO_3$ is very similar to the development of FC austenite phase in the present sample. The fraction of metastable FM phase at low temperature increases with increasing H and it was observed that beyond a certain value of H (above 60 kOe for $Nd_{0.5}Sr_{0.5}MnO_3$), the CO state gets completely molten. These manganite samples also show similar thermomagnetic irreversibility between the FC and ZFC measurements.[20,21]

The irreversibility between temperature dependence of FC and ZFC magnetization is quite common in case of glassy magnetic materials. This is attributed to the random freezing of the spins during the zero-field-cooling. The ZFC state is a nonequilibrium state and it approaches the FC state with time $[M_{ZFC}(t\rightarrow\infty)\approx M_{FC}]$.[22] In contrary to this, the FC state is found to be more metastable in case of $Ni_2Mn_{1.36}Sn_{0.64}$ than the ZFC one. As observed in Fig. 2, the FC ρ approaches the ZFC ρ on the heating branch once the field is removed. This is an example of *reentrant transition*, where by virtue of the zero-field heating of the field-cooled state up to above MT, a transition such as "arrested austenite" $(\mathcal{A}')\rightarrow$ "martensite" $(\mathcal{M})\rightarrow$ "austenite" $(\mathcal{A})$ occurs. The equivalent re-entrant transition in $(Nd,Sm)_{0.5}Sr_{0.5}MnO_3$ is the collapse of the arrested FM state into CO state on heating.

We observe strong time dependent effect of ρ in the FC state, which is practically absent in the ZFC state. This evidence of metastability of the FC state can be due to some arrested austenite fraction, which gradually converts to martensite with time. Another likely source of this metastability is the preferential nucleation of martensite under an applied magnetic field. Recently, Aksoy *et al.*[23] have reported the result of their T-dependent strain measurements in presence of H in several Ni-Mn-X (X=In,Sn,Sb,Ga) based FSMAs. It is observed that during cooling through M_S in presence of H, the martensite variants are grown with their easy axis of magnetization directed along the direction of applied field. However, growth is random when the sample is cooled in zero field. The observed relaxation in the FC state of the present sample can be related to this preferential nature of the variant growth. When the field is removed below M_S, the oriented variants tend to get randomized by the thermal energy with time. The randomized variants would offer more resistance due to the enhanced scattering of electrons from the interfaces and as a result a time dependent increase of resistance is expected.

The thermal hysteresis observed in the present sample around the MT is inherently related to the supercooling and superheating of high-T and low-T phases, respectively. In the standard notation of first-order phase transition, the extent of metastability is bound between the temperatures, T^{**} and T^{*}.[24] In case of MT, the temperatures M_F and A_F are equivalent to T^{*} and T^{**}, respectively. Below T^{*}, the supercooled state becomes unstable, and the system completely transform into low-T phase. Similarly, above T^{**}, the superheated state cannot survive. In real system, the presence of disorder and/or impurity can locally reduce the free-energy barrier, causing the low-T (or high-T) phase to nucleate even above T^{*} while cooling (or below T^{**}while heating).[25] Therefore, one can have phase coexistence in the region of hysteresis.[9] Polycrystalline sample such as $Ni_2Mn_{1.36}Sn_{0.64}$ is expected to possesses disorder/defects, and it will have both high-T austenitic and low-T martensitic phases in the region around MT where the thermal hysteresis is observed. With increasing H, ρ decreases (and simultaneously M increases) gradually, signaling monotonic increase of austenitic fraction at the expense of martensite. This is quite different from the sharp field-induced transition at a critical field in case of Gd_5Ge_4,[26] RCo_2 (R=rare earth) Laves phase compounds,[27] or B-site doped Perovskite oxides.[28] Possibly, in case of Mn-based Heusler alloys, the application of H in the region of transition, causes the free-energy barrier to decrease. The higher the magnetic field, the effect on the free-energy barrier is stronger, causing the development of more austenite by thermal activation. In other words, the austenite does not equilibrate with the sudden collapse of the barrier at a critical field. In addition, disorder gives a spatial variation of the free-energy profile, as a result, the threshold field for the martensite to austenite transition will vary over the sample. In effect, this will cause a gradual melting of the martensite with increasing H.

However, the above picture of first-order phase transition is inadequate to account for the complex H-T phase diagram in $Ni_2Mn_{1.36}Sn_{0.64}$. Considering the fact that T^{*} (or M_F) denotes the end point of metastability in the low-T side, one would not expect the formation of arrested state well below M_F. In addition, the Zeeman energy term ($-MH$) is too weak to play a significant role for a large change in M_S under H. We need to remember that in the present case the elastic strain and magnetization are closely interconnected. Landau free energy (F_L) with biquadratically coupled order parameters has been used for magnetostructural transition in manganites such as $La_{1-x}Sr_xMnO_3$ and $Nd_{0.5}Sr_{0.5}MnO_3$.[8,19,20] A similar model can be appropriate in the present case, where

$$F_L = f_0 + \alpha(T-T_C)M^2 + \beta M^4 - MH + \alpha'(T-T_0)\sigma^2 + \beta'\sigma^4 + \gamma'\sigma^6 + \lambda M^2\sigma^2. \quad (1)$$

Here, M and σ (strain) are two order parameters corresponding to second-order ferromagnetic transition and first-order MT, respectively. The term $\lambda M^2\sigma^2$ denotes the coupling between magnetic and elastic energies and $-MH$ is the Zeeman energy term. This free energy can bear the high-temperature ferromagnetic ordering (at T_C) and austenite to martensite transition (at T_0). However, for suitable values of the coefficients, it can give rise to a first-order transition line, where the free-energy minimum for the martensite is low enough for structural ordering, and a metastable austenite (a metallic ferromagnetic state in case of manganite) prevails down to low temperatures.[29] In the present case, this undercooled austenite phase might be primarily responsible for the lower ρ and higher M in the field-cooled state of the sample.

In this connection, we would like to mention that the martensitic transition temperatures of $Ni_2Mn_{1+x}Sn_{1-x}$ alloys depend strongly on Mn concentration. It is believed that the excess Mn (denoted by x) gives rise to some short-range antiferromagnetic (AFM) correlations in the system and it plays an important role for the structural instability.[30] M_S shifts to higher T by 80 K for x changing from 0.36 (present sample) to 0.4. The x=0.4 sample also shows irreversibility in the ρ (and also M) versus H behavior in the region of MT due to field-induced transition, however, the presence of undercooled austenite phase in the FC data down to lowest temperature is absent here.[13] For x=0.4, the FC ρ approaches to the ZFC ρ as the temperature is lowered below the M_F of the sample. The MT occurs at much higher temperature in case of x=0.4, and possibly in presence of thermal fluctuations at relatively high T, the undercooled austenite cannot be stabilized here.

V. SUMMARY AND CONCLUSION

We have investigated the metastability associated with the structural transition in $Ni_2Mn_{1.36}Sn_{0.64}$ by carefully controlling the parameters such as magnetic field and temperature. The thermally driven martensitic transition is strongly influenced by the applied magnetic field. We observe a remarkable *H-T* phase diagram, where an undercooled austenite phase exists down to the lowest temperature. We have mooted the concept of coupled order parameter for the present sample, which predicts an undercooled state in certain situations. A notable similarity is seen between the present phenomenon with some manganites such as, $Nd_{0.5}Sr_{0.5}MnO_3$, showing first-order transition from ferromagnetic to charge-order state. The microscopic origin of the magnetic and structural aspects in Heusler alloys and manganites are quite different. The commonality in their bulk properties possibly lies to the fact that a generic statistical model for magnetostructural transition with two competing order parameters is obeyed by both the systems. It should be borne in mind that both manganites and the present FSMA are phase separated systems and AFM correlations play an important role toward the structural instability in both the systems.

The paramagnetic to FM and FM to CO transitions in $Nd_{0.5}Sr_{0.5}MnO_3$-derived compositions show strong hydrostatic pressure (P) effect. It can be equally interesting to investigate the effect of P on the sample and construct the *P-T* phase diagram, which will bring out correctness of the coupled model and will through more light on the fate of the metastable state under pressure.

ACKNOWLEDGMENT

We acknowledge the financial support from CSIR, India for the present work.

*sspsm2@iacs.res.in

[1] K. A. Gschneidner, Jr., V. K. Pecharsky, and A. O. Tsokol, Rep. Prog. Phys. **68**, 1479 (2005).
[2] L. Morellon, P. A. Algarabel, M. R. Ibarra, J. Blasco, B. García-Landa, Z. Arnold, and F. Albertini, Phys. Rev. B **58**, R14721 (1998).
[3] R. Kainuma, Y. Imano, Y. Sutou, H. Morito, S. Okaoto, O. Kitakam, K. Oikawa, A. Fujita, T. Kanomata, and K. Ishta, Nature (London) **439**, 957 (2006).
[4] T. Krenke, E. Duman, M. Acet, E. F. Wassermann, X. Moya, L. Mañosa, A. Planes, E. Suard, and B. Ouladdiaf, Phys. Rev. B **75**, 104414 (2007).
[5] L. Morellon, J. Stankiewicz, B. García-Landa, P. A. Algarabel, and M. R. Ibarra, Appl. Phys. Lett. **73**, 3462 (1998).
[6] P. A. Algarabel, M. R. Ibarra, C. Marquina, and A. del Moral, Appl. Phys. Lett. **66**, 3061 (1995).
[7] V. Sechovsky, L. Havela, K. Prokes, H. Nakotte, F. R. de Boer, and E. Brúck, J. Appl. Phys. **76**, 6913 (1994).
[8] A. Asamitsu, Y. Moritomo, R. Kumai, Y. Tomioka, and Y. Tokura, Phys. Rev. B **54**, 1716 (1996).
[9] For a review, see S. B. Roy and P. Chaddah, Phase Transitions **77**, 767 (2004).
[10] J. Enkovaara, A. Ayuela, A. T. Zayak, P. Entel, L. Nordstrom, M. Dubee, J. Jalkanen, J. Impola, and R. M. Nieminen, Mater. Sci. Eng., A **378**, 52 (2004).
[11] Y. Sutou, Y. Imano, N. Koeda, T. Omori, R. Kainuma, K. Ishida, and K. Oikawa, Appl. Phys. Lett. **85**, 4358 (2004).
[12] T. Krenke, M. Acet, E. F. Wassermann, X. Moya, L. Mañosa, and A. Planes, Nat. Mater. **4**, 450 (2005).
[13] S. Chatterjee, S. Giri, S. Majumdar, and S. K. De, Phys. Rev. B **77**, 012404 (2008).
[14] K. Koyama, K. Watanabe, T. Kanomata, R. Kainuma, K. Oikawa, and K. Ishida, Appl. Phys. Lett. **88**, 132505 (2006).
[15] V. K. Sharma, M. K. Chattopadhyay, and S. B. Roy, Phys. Rev. B **76**, 140401(R) (2007).
[16] R. Street and S. D. Brown, J. Appl. Phys. **76**, 6386 (1994).
[17] W. Eerenstein, N. D. Mathur, and J. F. Scott, Nature (London) **442**, 759 (2006).
[18] C. Pfleiderer, M. Uhlarz, S. M. Hayden, R. Vollmer, H. v. Löhneysen, N. R. Bernhoeft, and G. G. Lonzarich, Nature (London) **412**, 58 (2001).
[19] Y. Tokura, H. Kuwahara, Y. Moritomo, Y. Tomioka, and A. Asamitsu, Phys. Rev. Lett. **76**, 3184 (1996).
[20] H. Kuwahara, Y. Moritomo, Y. Tomioka, A. Asamitsu, M. Kasai, R. Kumai, and Y. Tokura, Phys. Rev. B **56**, 9386 (1997).
[21] R. Rawat, K. Mukherjee, Kranti Kumar, A. Banerjee, and P. Chaddah, J. Phys.: Condens. Matter **19**, 256211 (2007).
[22] J. A. Mydosh, *Spin Glasses: An Experimental Introduction* (Taylor & Francis, London, 1993), p. 69.
[23] S. Aksoy, T. Krenke, M. Acet, and E. F. Wassermann, Appl. Phys. Lett. **91**, 251915 (2007).
[24] P. Chaikin and T. Lubensky, *Principles of Condensed Matter Physics* (Cambridge University Press, Cambridge, 1995).
[25] S. Chatterjee, S. Giri, S. Majumdar, A. K. Deb, S. K. De, and V. Hardy, J. Phys.: Condens. Matter **19**, 346213 (2007).
[26] E. M. Levin, K. A. Gschneidner, Jr., and V. K. Pecharsky, Phys. Rev. B **65**, 214427 (2002).
[27] E. Gratz and A. S. Markosyan, J. Phys.: Condens. Matter **13**, R385 (2001).
[28] R. Mahendiran, A. Maignan, S. Hébert, C. Martin, M. Hervieu, B. Raveau, J. F. Mitchell, and P. Schiffer, Phys. Rev. Lett. **89**, 286602 (2002).
[29] Y. Imry, J. Phys. C **8**, 567 (1975).
[30] P. J. Brown, A. P. Gandy, K. Ishida, R. Kainuma, T. Kanomata, K. U. Neumann, K. Oikawa, B. Ouladdiaf, and K. R. A. Ziebeck, J. Phys.: Condens. Matter **18**, 2249 (2006).